Nuclear Science Computing Center at CCNU

In-medium Bottomonium Properties from Lattice NRQCD Calculations with Extended Meson Operators

Wei-Ping Huang
Central China Normal University

in collaboration with
Heng-Tong Ding, Rasmus Larsen, Stefan Meinel, Swagato Mukherjee, Peter Petreczky

The 9th International Symposium on Heavy Flavor Production
in Hadron and Nuclear Collisions (HF-HNC 2024), Dec. 6 - 11, 2024 @ Guangzhou

Quarkonium as a probe

Quarkonium suppression via color screening in Quark-Gluon Plasma

T. Matsui, H. Satz, PLB178 (1986) 416

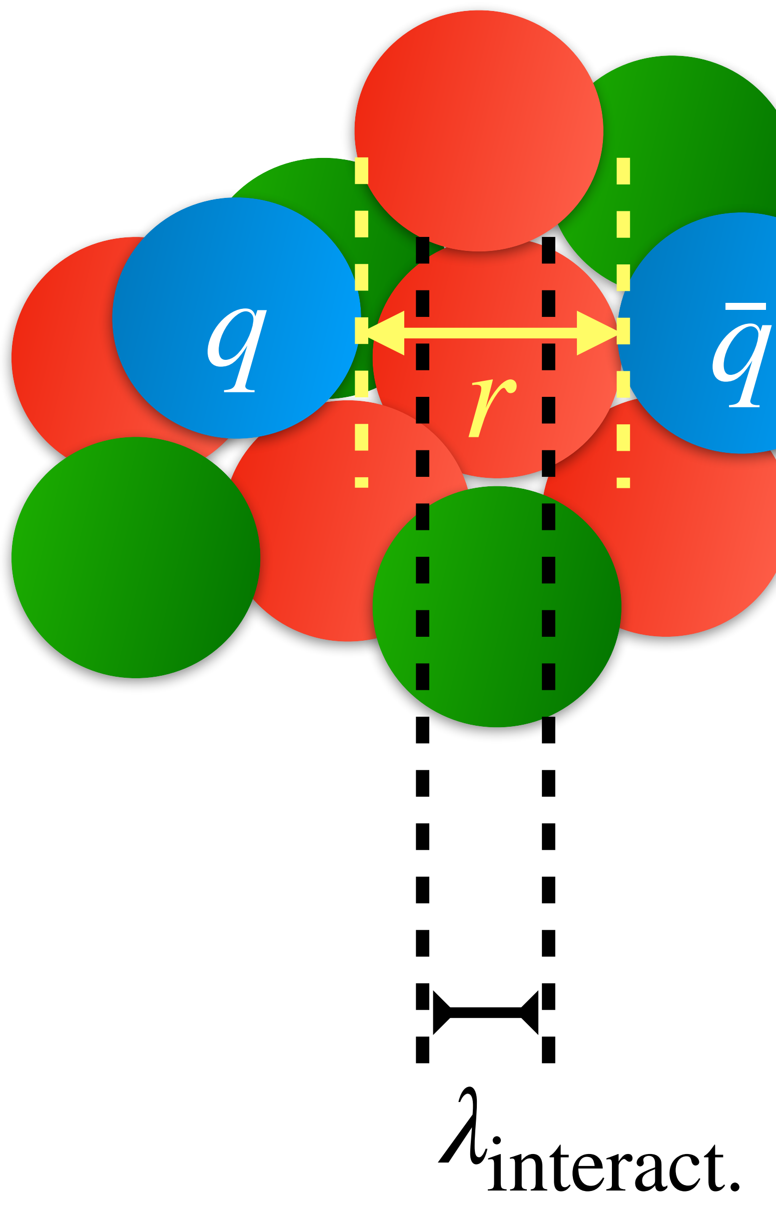

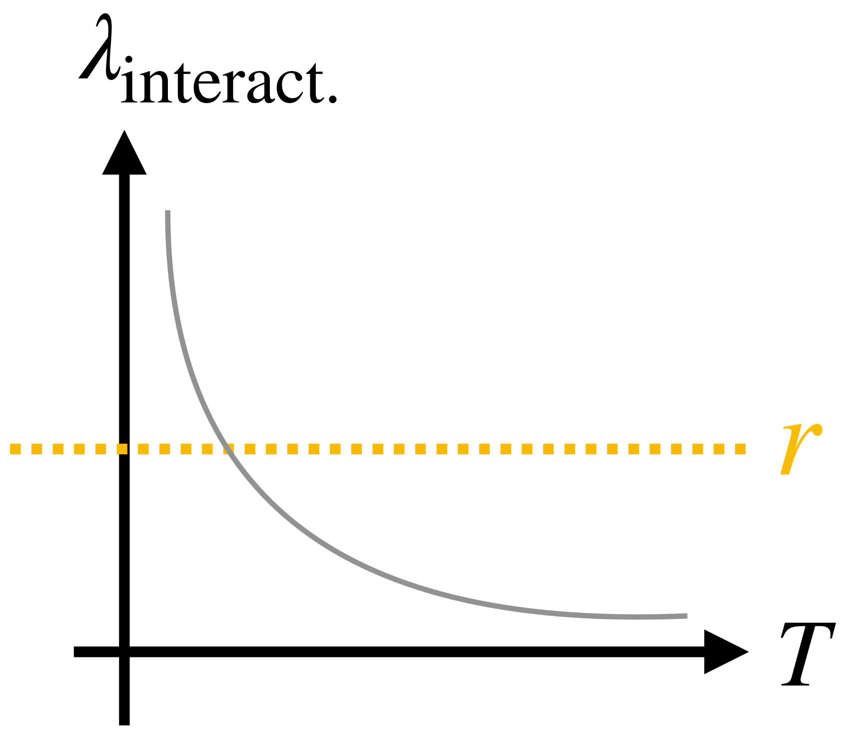

Sequential in-medium modifications at finite temperatures in experiments

Sequential dissolution

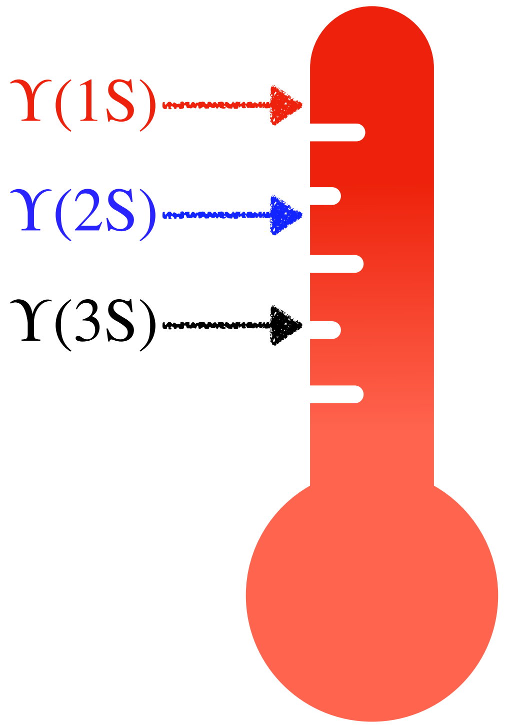

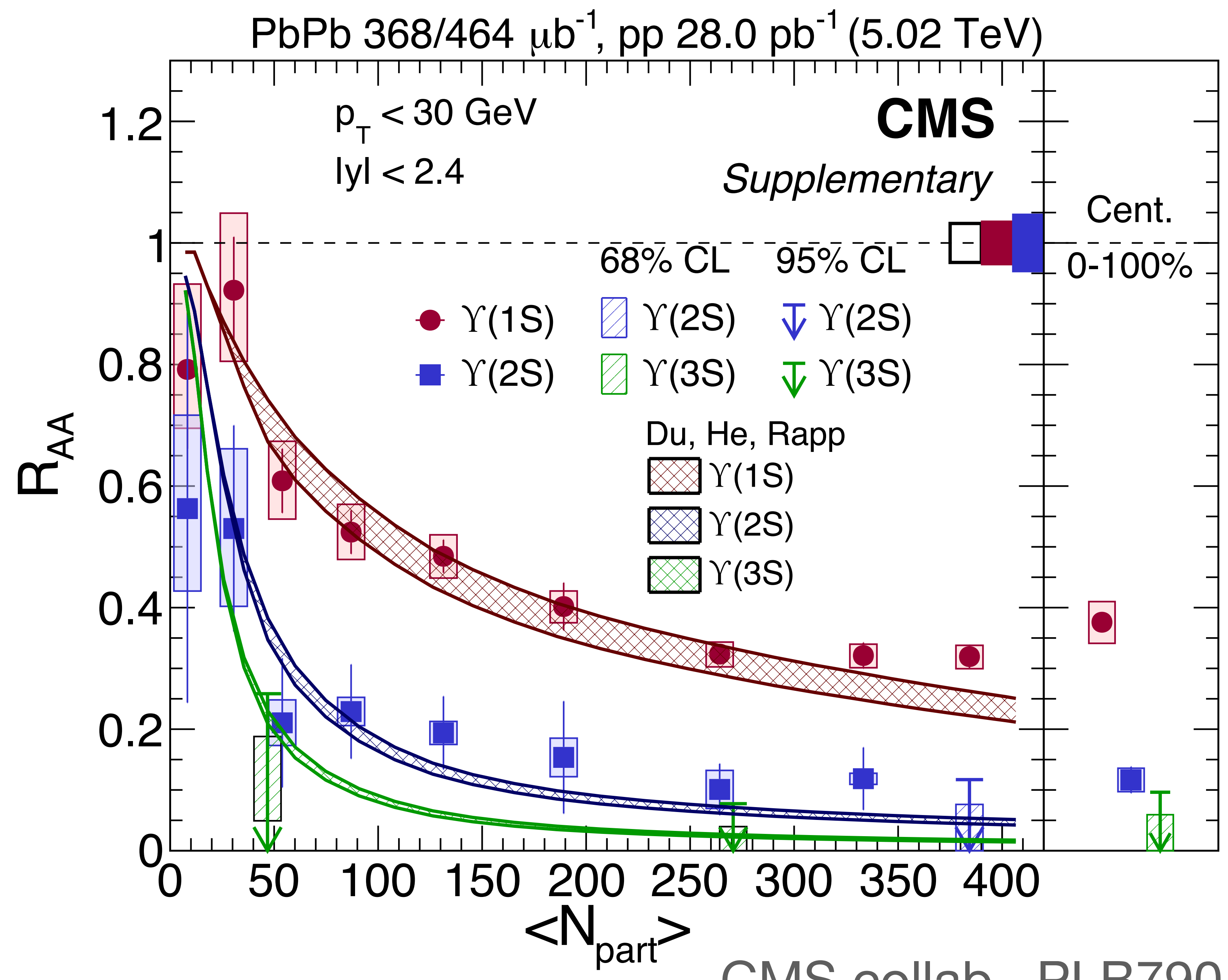

CMS collab., PLB790 (2019) 270

In-medium quarkonium properties are encoded in spectral function, related to Euclidean correlators calculable on the lattice:

$$C(\tau, T) = \int_{-\infty}^{+\infty} \mathrm{d}\omega \; \rho(\omega, T) K(\tau, \omega, T)$$

Motivation: why Lattice NRQCD + extended sources

Relativistic QCD

- Limited sensitivity in $C(\tau, T)$: $\tau_{\max} = 1/(2T)$

  A. Mocsy, P. Petreczky, PRD 77, 014501(2008)
  P. Petreczky, EPJC 62, 85 (2009)

- Large discretization effects $\sim aM_b$

Point source

- $C(\tau, T)$ at large τ are needed for lack of overlap with specific state
- Non-optimal overlap with excited states

Non-relativistic QCD + **Extended source**

- Heavy quark mass scale is integrated out
- Pair creation is not allowed $\Rightarrow \tau_{\max} = 1/T$

  N. Brambilla, J. Ghiglieri, et.al., PRD 78, 014017(2008)

- Better projection onto particular state

  R. Larsen, et.al., PRD 100, 074506 (2019)
  R. Larsen, et.al., PLB 800, 135119 (2020)

- Optimized for excited states

↓

☑ More sensitive to thermal effects

☑ Able to study sequential in-medium modifications shown in excited states

Correlators with extended sources

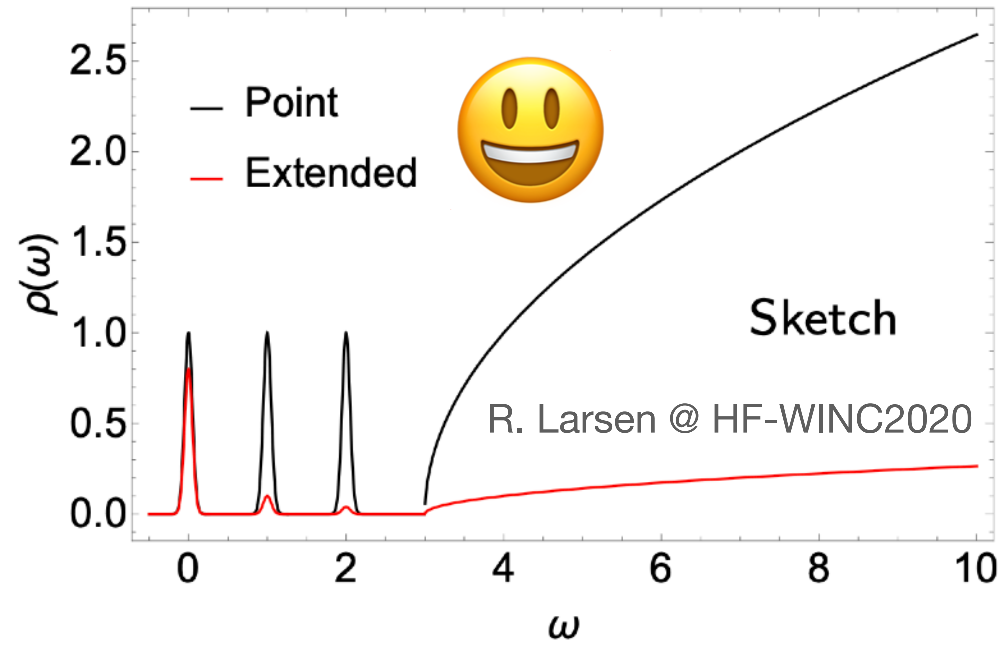

Correlator: $$C(\tau) = \sum_{\mathbf{x}} \langle O(\mathbf{x}, \tau) O^{\dagger}(\mathbf{0}, 0) \rangle$$

Gaussian-smeared source

R. Larsen, et.al., PRD 100, 074506 (2019)

$$O(\mathbf{x}, \tau) = \bar{\tilde{q}}(\mathbf{x}, \tau)\Gamma\tilde{q}(\mathbf{x}, \tau)$$

Bottomonium interpolators

Smeared quark and antiquark fields: $\tilde{q} = Wq$

Gaussian-shaped factor

Wave-function optimized source

R. Larsen, et.al., PLB 800, 135119 (2020)

$$O_\alpha(\mathbf{x}, \tau) = \sum_{\mathbf{r}} \Psi_\alpha(\mathbf{r})\bar{q}(\mathbf{x} + \mathbf{r}, \tau)\Gamma q(\mathbf{x}, \tau)$$

From the discretized 3-d Schrodinger equation:

$$\left[-\frac{\Delta}{m_b} + V(\mathbf{r})\right]\Psi(\mathbf{r}) = E\Psi(\mathbf{r})$$

$O(a^4)$-improved discretized Laplacian

Cornell potential

S. Meinel, PRD 82, 114502 (2010)

Simulation Details

- Bottom quark on the lattice:

S. Meinel, PRD 82, 114502 (2010)

R. Larsen, et.al., PRD 100, 074506 (2019)

R. Larsen, et.al., PLB 800, 135119 (2020)

— Tree-level tadpole-improved NRQCD action, with $\mathcal{O}(v^6)$ corrections

— Bare bottom mass tuning: matching kinetic mass M_{kin,η_b} to its PDG value, leading to $aM_b = 0.955(17)$

- Background gauge fields with (2+1)-flavor dynamical sea quarks:

— HISQ/tree action

— Quark mass: $m_s^{\mathrm{phy}}/m_l = 20$ $(m_\pi \approx 160$ MeV$)$

— Two fixed finer lattice spacings: $a = 0.0493$ fm and 0.0602 fm

— Temperature is increased by reducing the temporal extent: $N_\tau \in [16,\ 30]$, $T \in (133,\ 250)$ MeV

Results in Vacuum: effective mass

$$M_{\text{eff}}(\tau) = \frac{1}{a} \log \left[\frac{C(\tau, T)}{C(\tau + a, T)} \right]$$

All vertical scales are calibrated with the spin-averaged mass of 1S bottomonium hereafter

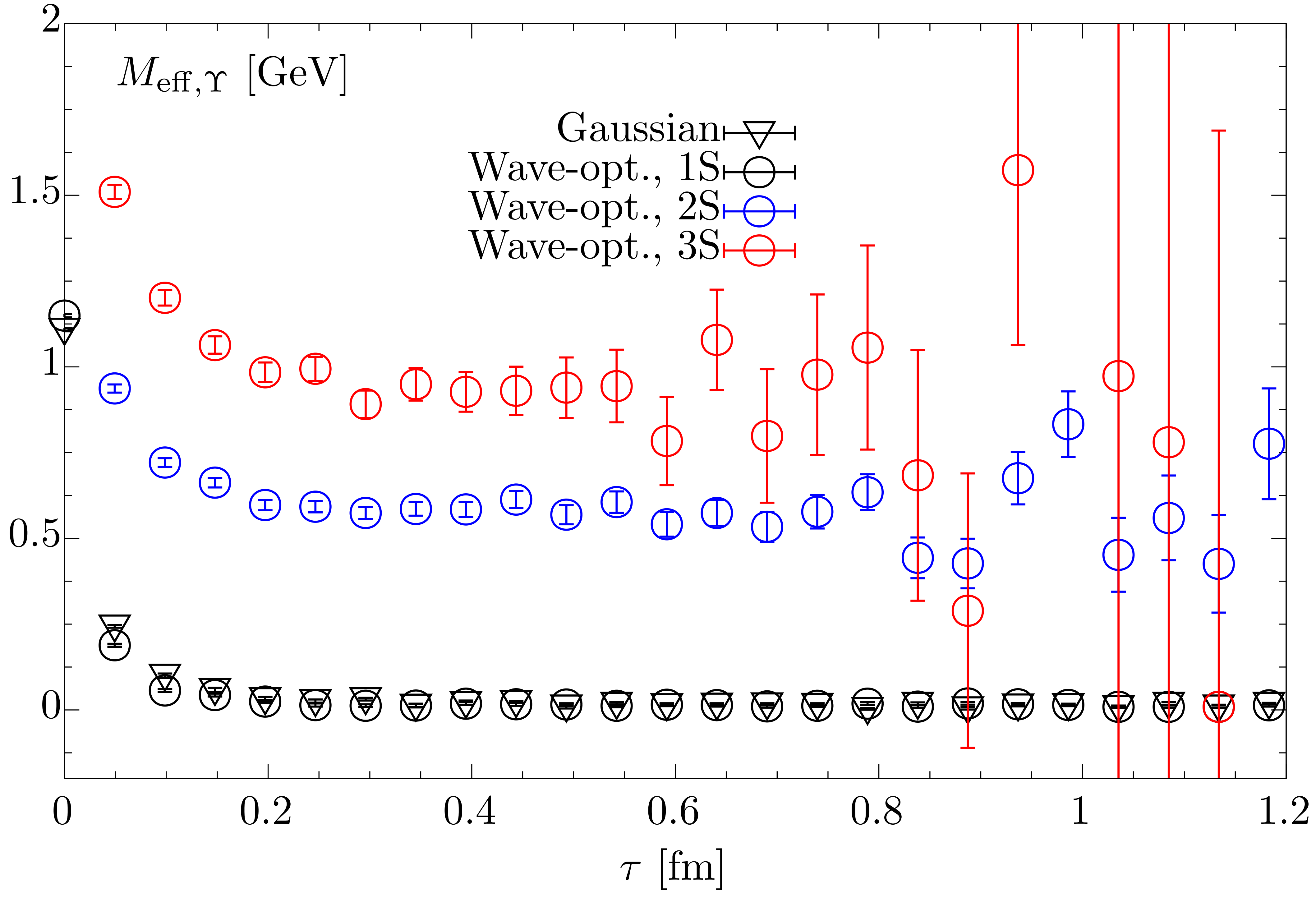

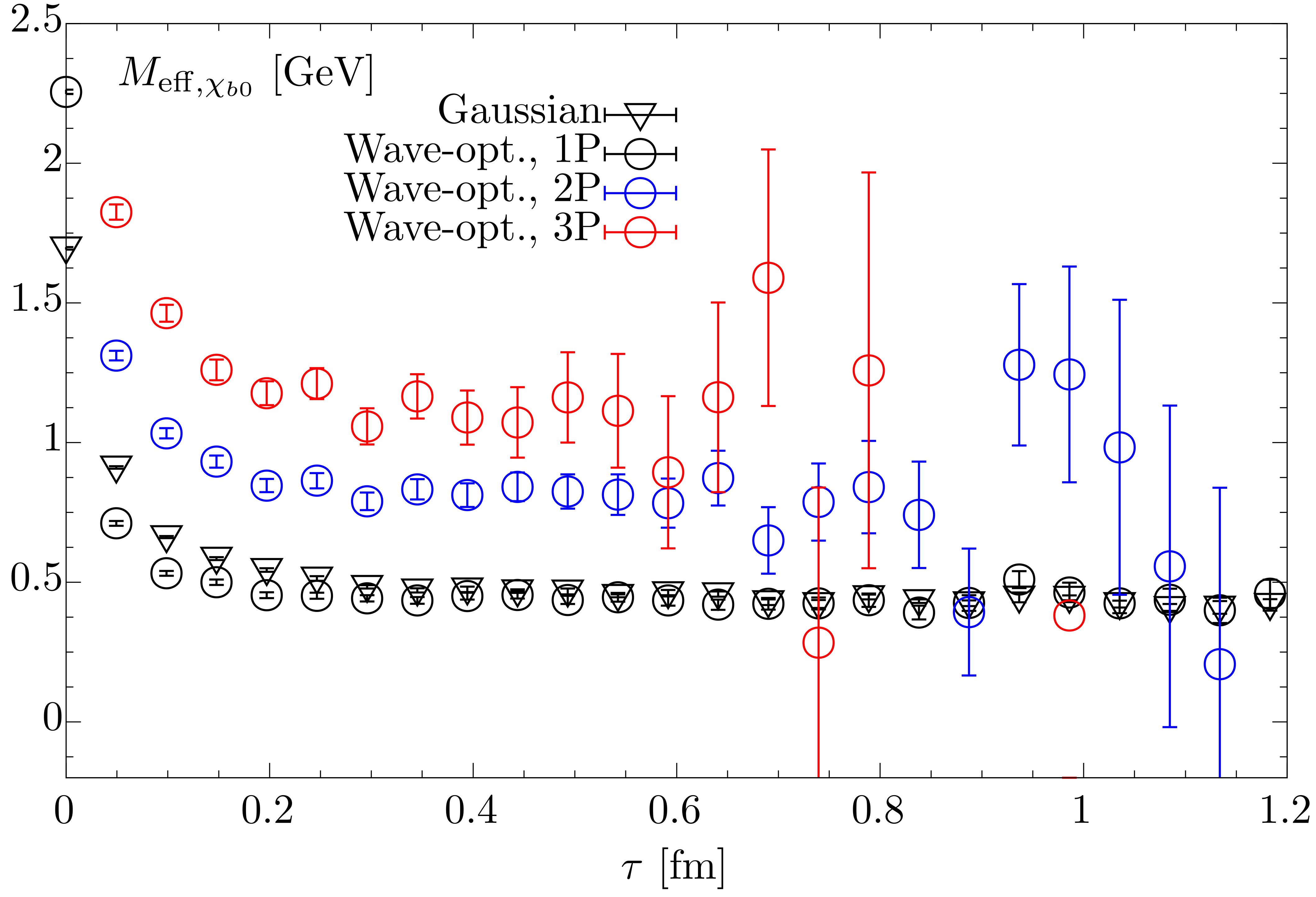

- Mild effects from different extended sources for ground states
- Plateau region from $\tau \sim 0.25$ fm, shorter for excited states with worse SNR

Results in Vacuum: mass spectra

Mass difference: $\Delta M = M - (M_{\eta_b} - 3M_{\Upsilon})/4$

Spin-averaged mass of 1S bottomonium

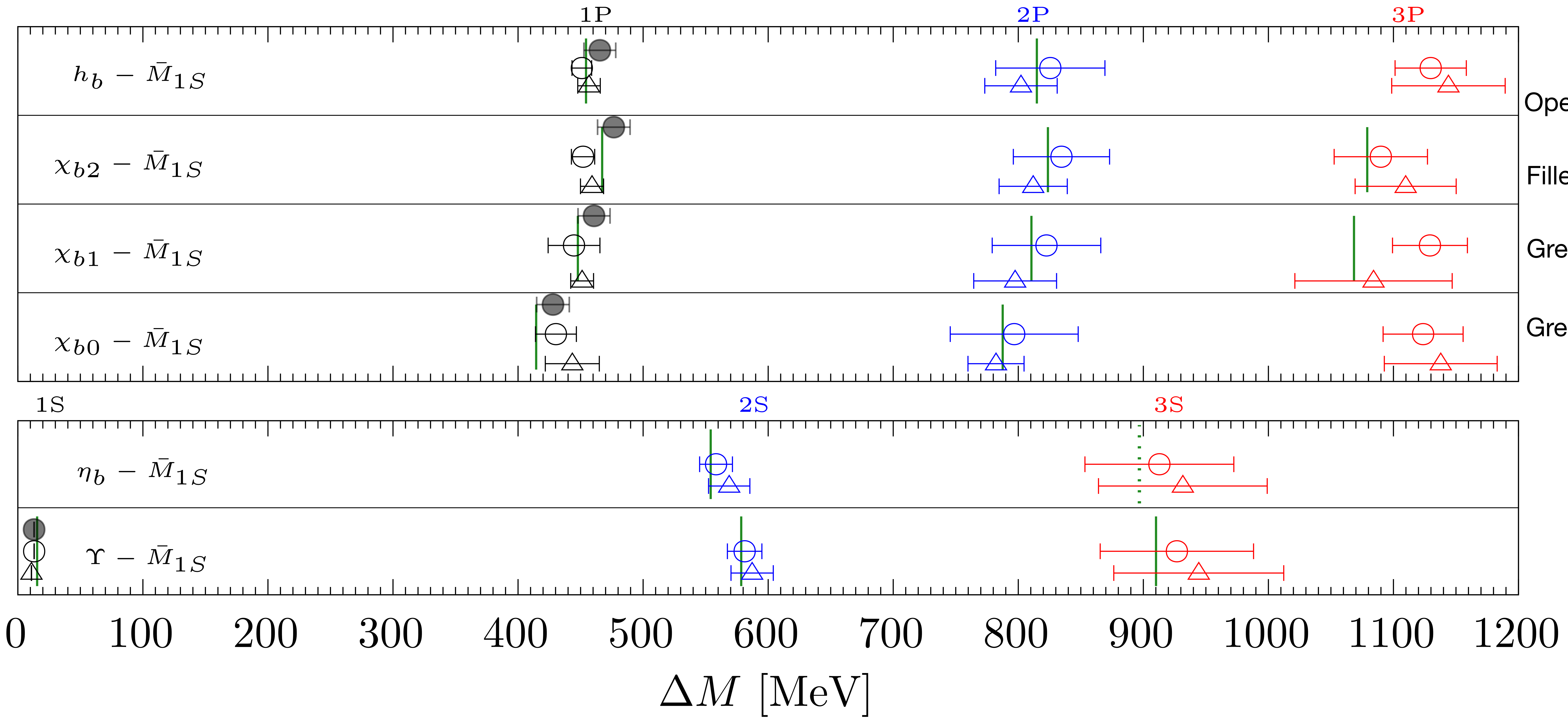

Open points: wave-function optimized results

Filled points: Gaussian-smeared results

Green solid line: PDG values

Green dashed line: lattice-predicted $M_{\eta_b(3S)}$

R. Larsen, et.al., PLB 800, 135119 (2020)

Results at finite temperatures: effective mass

Measured with Gaussian-smeared sources

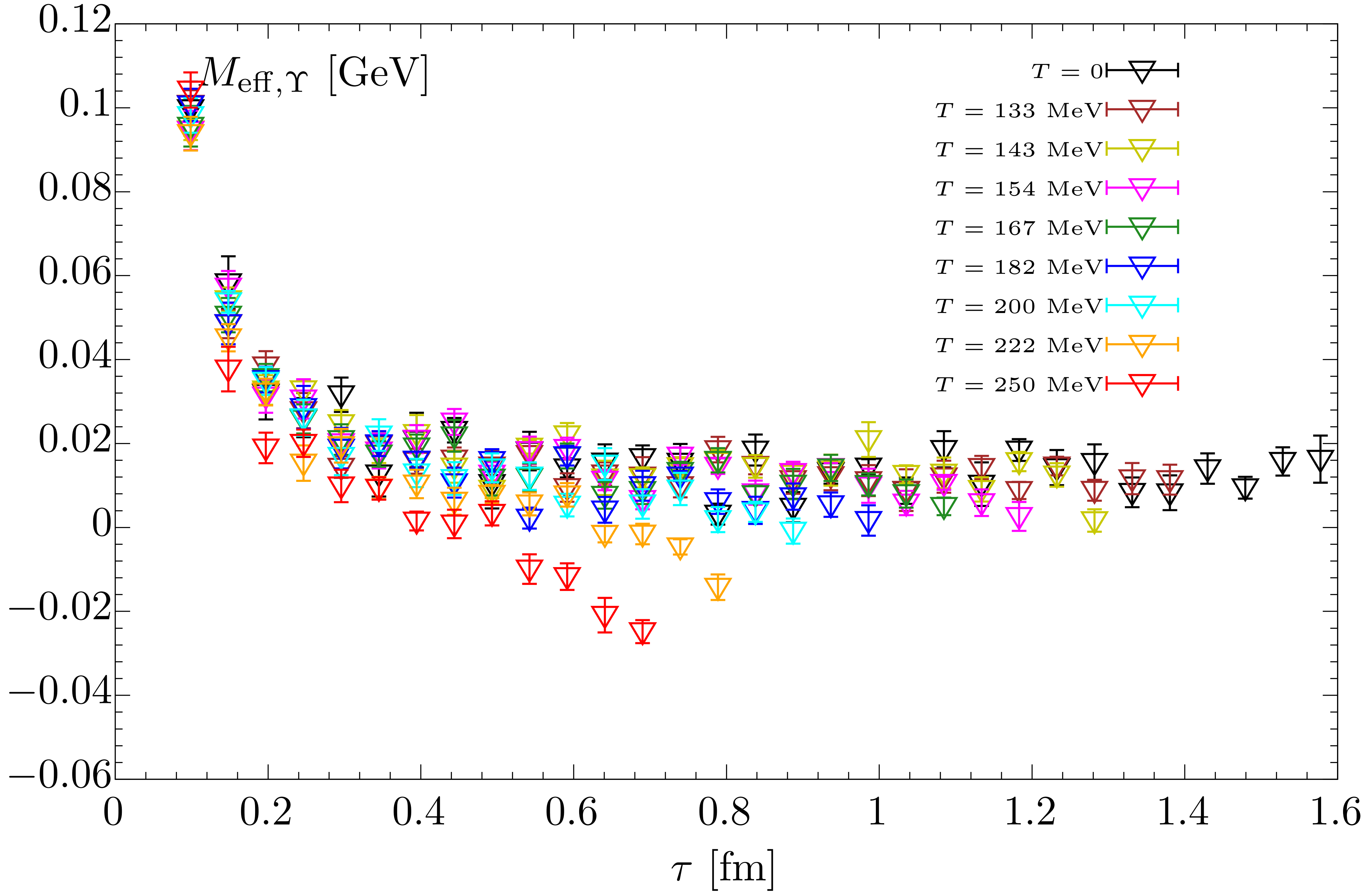

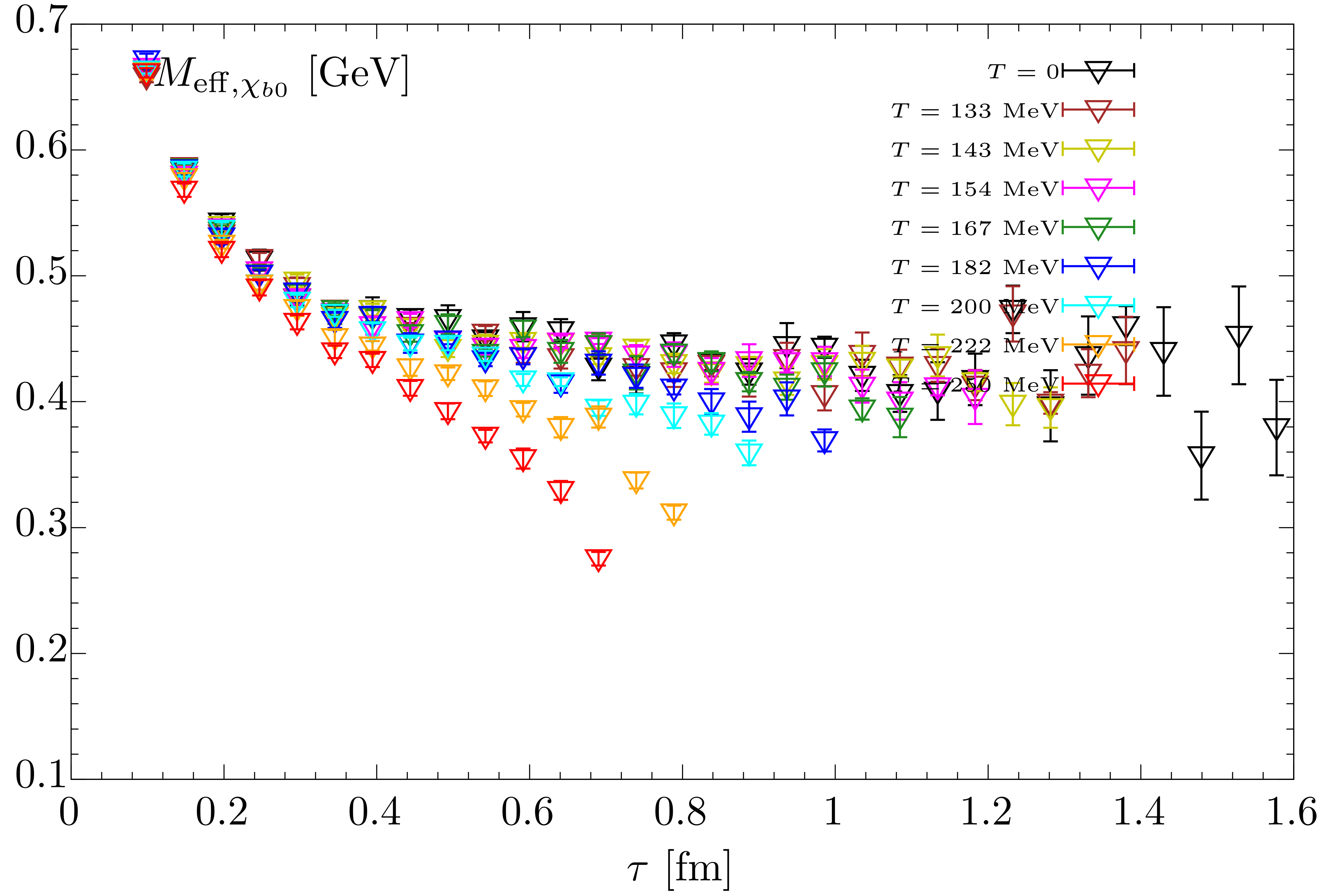

- Overlaps within small τ: mild temperature dependence
- As T increases: plateau ends at shorter τ, followed by a faster drop at the tail
- Earlier onset of fall-off and steeper slope: P-wave channels are more sensitive to thermal effects

Results at finite temperatures: effective mass

Measured with wave-function optimized sources

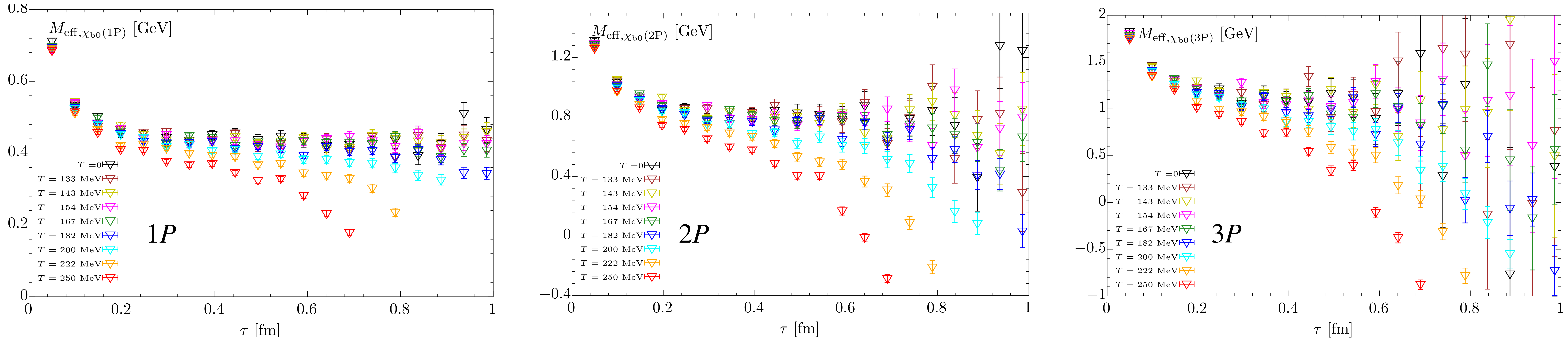

- Steeper slope at tail for higher excited state, with shorter and shorter plateau
- High excited states are more sensitive to thermal modifications

Continuum-subtracted correlator

$$C(\tau, T) = \int_{-\infty}^{+\infty} \mathrm{d}\omega\ \rho(\omega, T) e^{-\tau\omega}$$

$$\rho(\omega, T) = \rho_{\mathrm{med}}(\omega, T) + \rho_{\mathrm{cont}}(\omega)$$

Extended sources lead to
selective overlap with particular states:

In vacuum $\rho_{\mathrm{med}}(\omega, T=0) = A\delta(\omega - M)$

Mass of a state
targeted for projection

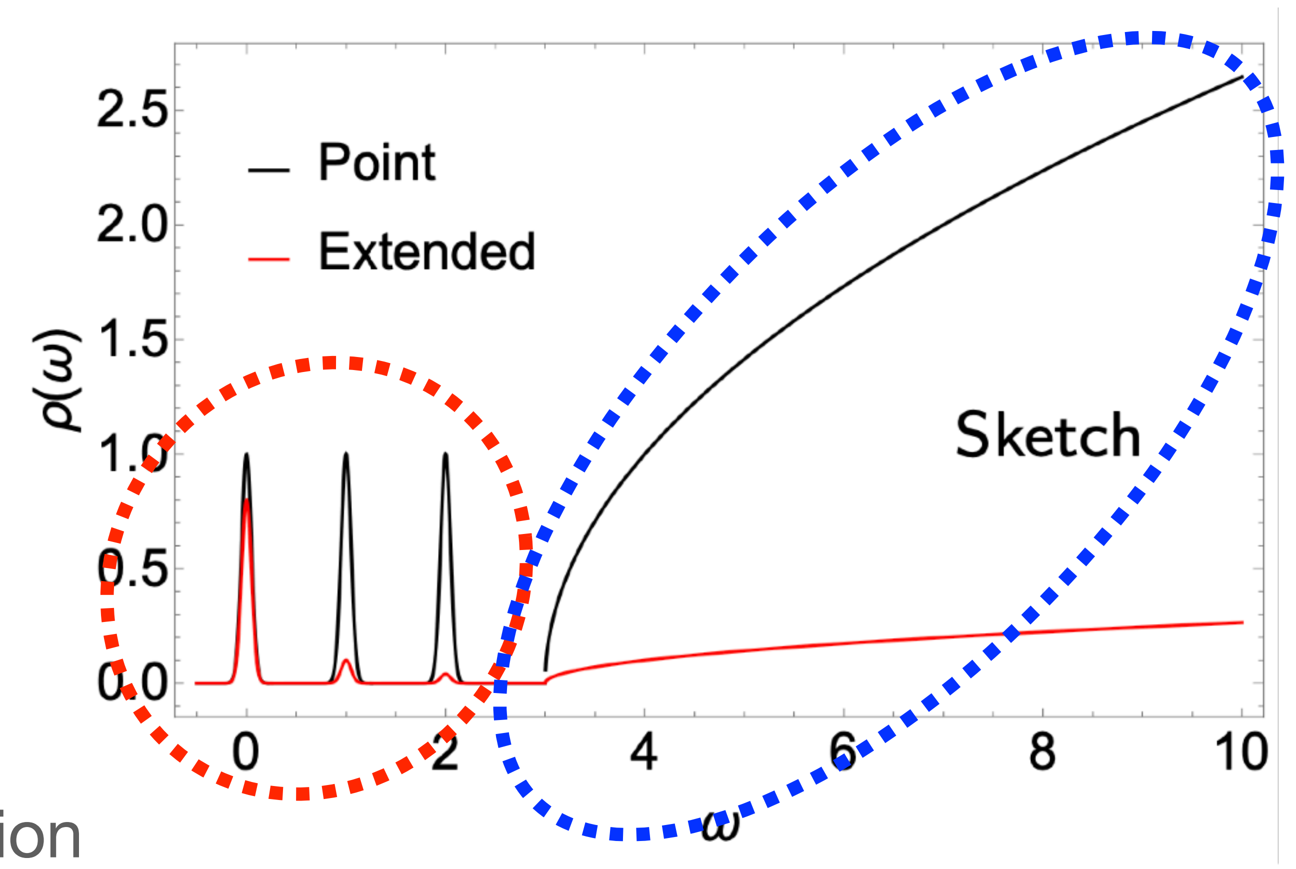

Temperature independent:
consistent with small τ behaviors in M_{eff}

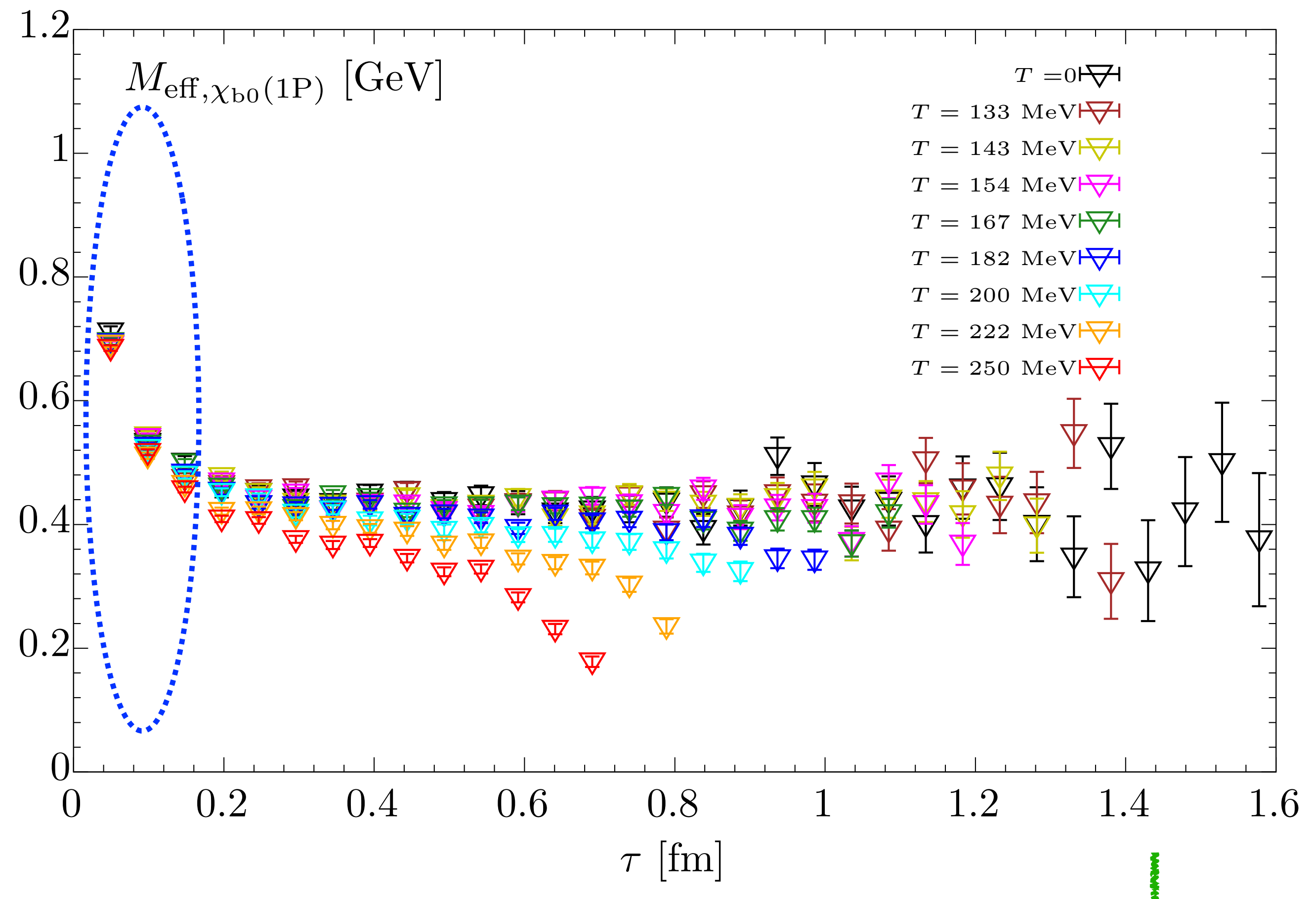

Extract continuum part at zero temperature: $C_{\mathrm{cont}}(\tau) = C(\tau, T=0) - Ae^{-M\tau}$

Define continuum-subtracted correlator: $C_{\mathrm{sub}}(\tau, T) = C(\tau, T) - C_{\mathrm{cont}}(\tau)$

Continuum-subtracted effective mass

Measured with Gaussian-smeared sources
(similar results for wave-function optimized sources)

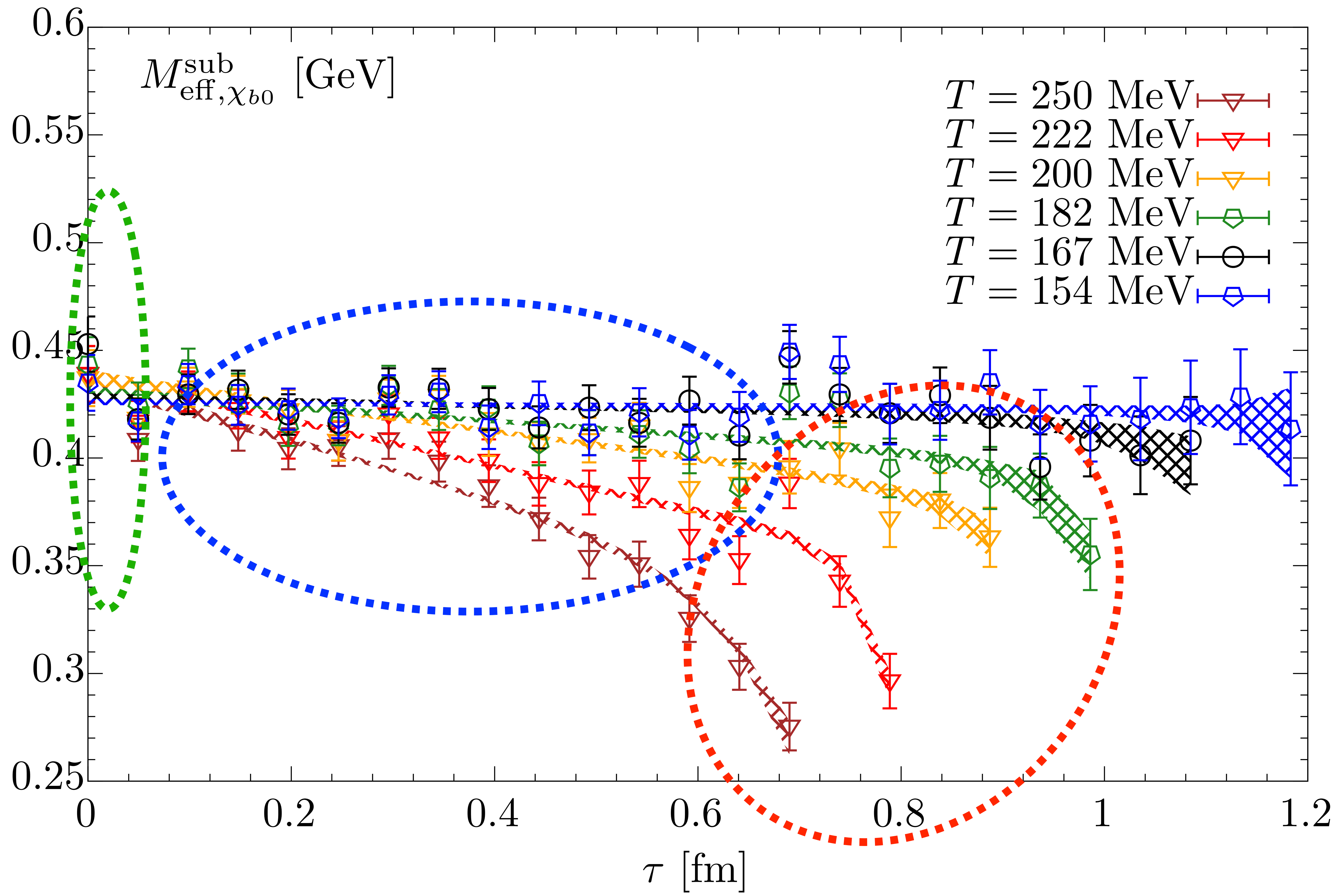

$$M^{sub}_{eff}(\tau) = \frac{1}{a}\log\left[\frac{C_{sub}(\tau,T)}{C_{sub}(\tau+a,T)}\right]$$

Small τ region:
close to bottomonium masses in vacuum

Middle τ region:
nearly linear decrease;
steeper slope for higher T

Tail around $\tau \sim 1/T$:
sharp drop

$$\rho_{med}(\omega,T) = \rho^{peak}(\omega,T) + A_{cut}(T)\delta\left(\omega - \omega_{cut}(T)\right)$$

Dominant peak,
related to linear behavior of M^{sub}_{eff} in middle τ

Small, medium-dependent contribution below the main peak,
related to M^{sub}_{eff} at large τ around $1/T$

Next: Extract in-medium parameters from $C^{sub}(\tau,T)$ via physically-motivated parameterization of $\rho^{peak}(\omega,T)$

Parameterization of $\rho^{\text{peak}}(\omega, T)$

Gaussian type: $$\rho_{\text{med}}(\omega,T) = A_{\text{med}}(T)\exp\left(-\frac{[\omega - M_{\text{med}}(T)]^2}{2\Gamma^2_{\text{med}}(T)}\right) + A_{\text{cut}}(T)\delta\left(\omega - \omega_{\text{cut}}(T)\right)$$

R. Larsen, et.al., PRD 100, 074506 (2019)

R. Larsen, et.al., PLB 800, 135119 (2020)

☹ NOT physically motivated

Cut-Lorentzian type: $$\rho_{\text{med}}(\omega,T) = A_{\text{med}}(T)\frac{\Gamma_{\text{med}}(T)}{\left(\omega - M_{\text{med}}(T)\right)^2 + \Gamma^2_{\text{med}}(T)}\Theta(\text{cut} - |\omega - M|) + A_{\text{low}}(T)\delta\left(\omega - \omega_{\text{low}}(T)\right)$$

A. Bazavov, et.al., PRD 109, 074504 (2024)

- 😃 physically appealing
- ☹ Only valid closely around the main peak
- ☹ Tail behavior is badly described around cut position, leading to vaguely defined cut-dependent width

---

Smooth cut-Lorentzian type: $$\rho_{\text{med}}(\omega,T) = A_{\text{med}}(T)\frac{\Gamma(T)}{\left(\omega - M_{\text{med}}(T)\right)^2 + \Gamma^2(T)} + A_{\text{low}}(T)\delta\left(\omega - \omega_{\text{low}}(T)\right),$$

$$\Gamma(T) = \frac{1}{4}\left\{1 + \tanh\left[\frac{\omega - M_{\text{med}} + n\Gamma_{\text{med}}}{d}\right]\right\} \times \left\{1 - \tanh\left[\frac{\omega - M_{\text{med}} - n\Gamma_{\text{med}}}{d}\right]\right\}$$

n and d are inputs from T-matrix analysis, controlling the tail shape of dominant peak of spectral function

😃 Better described tail of main peak

S. Y. F. Liu&R. Rapp, PRC 97, 034918 (2018)

Z. D. Tang, et.al., arXiv:2411.09132

In-medium parameters: mass shift

$$\Delta M = M_{\text{med}}(T) - M(T=0)$$

- ΔM consistent with zero: almost no change in the in-medium masses
- Unscreened real part of heavy quark-antiquark potential is supported up to T = 250 MeV

In-medium parameters: thermal width

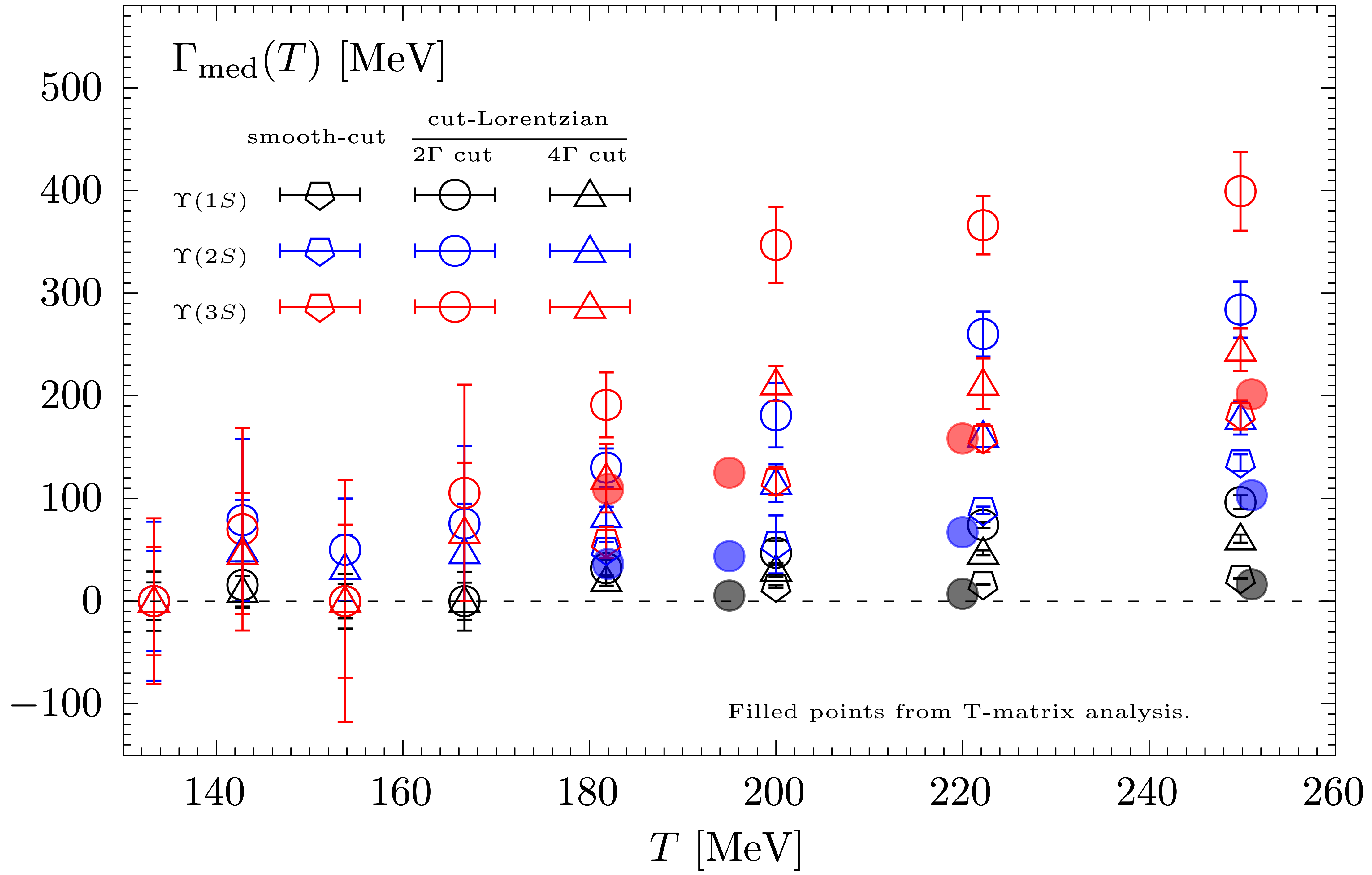

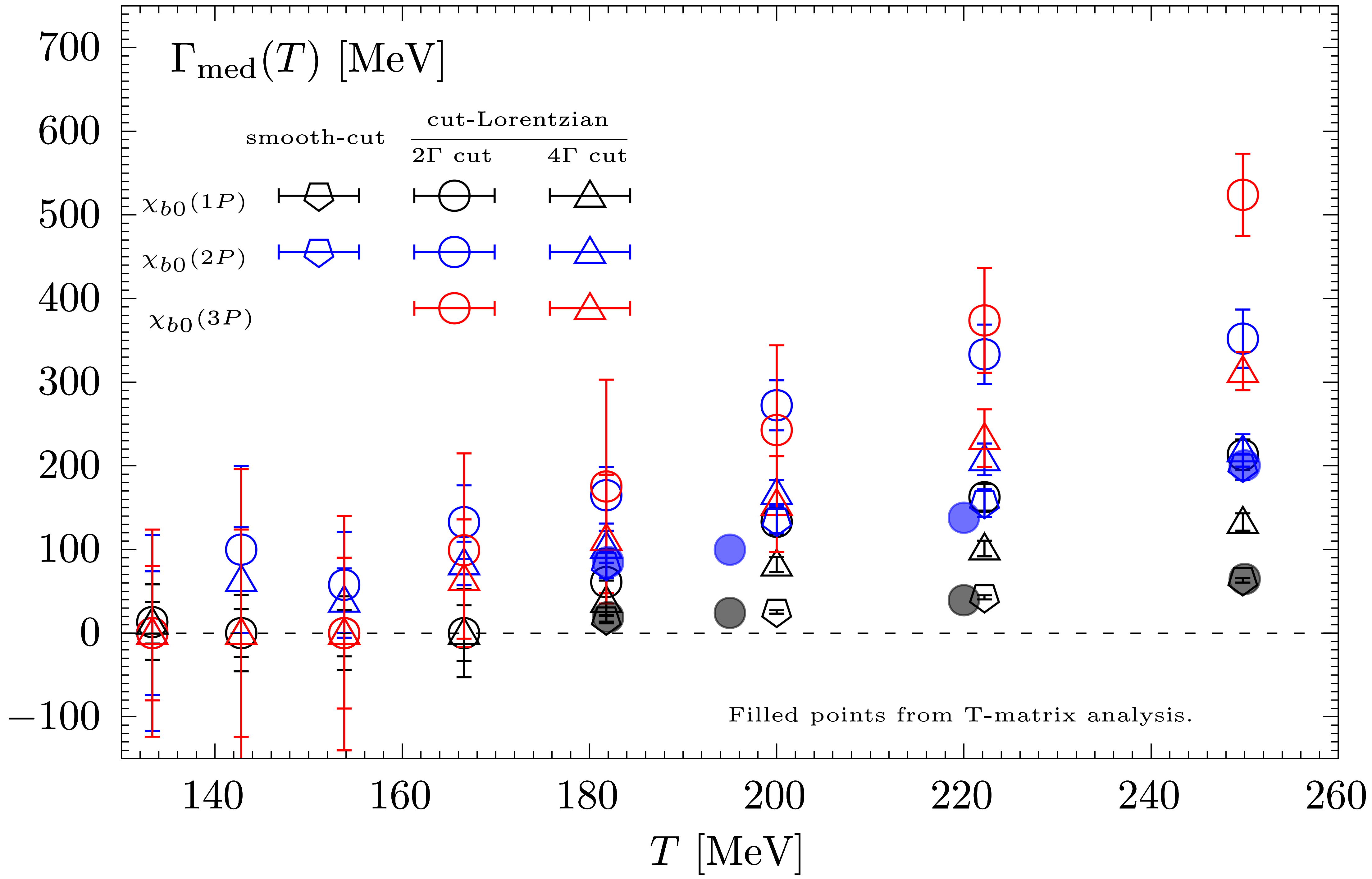

- Significant increasement with rising temperatures
- Sequential hierarchy appears in the magnitudes of the thermal widths
- Obvious cut-dependence in widths (tail of main peak matters!); consistency with T-matrix in smooth-cut
- Consistent with zero for $T < 180$ MeV based on current precision; constant fits are preferred
- Broadening spectral width leads to overlap of states and thus harder to be distinguished

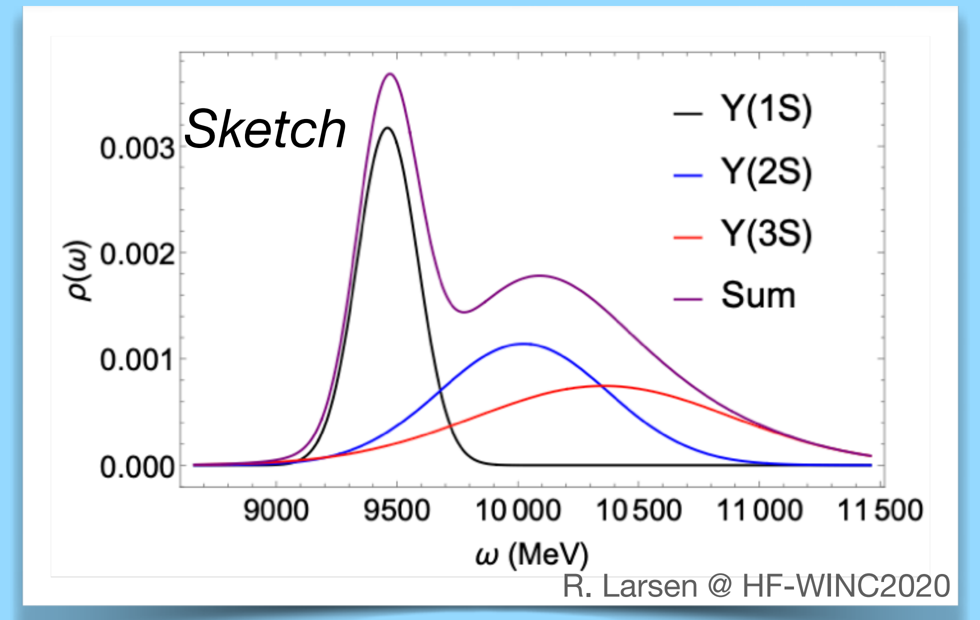

Summary

- From Lattice NRQCD calculations with two types of smeared sources within $T \in (133,250)$ MeV, temperature dependences in correlators are presented

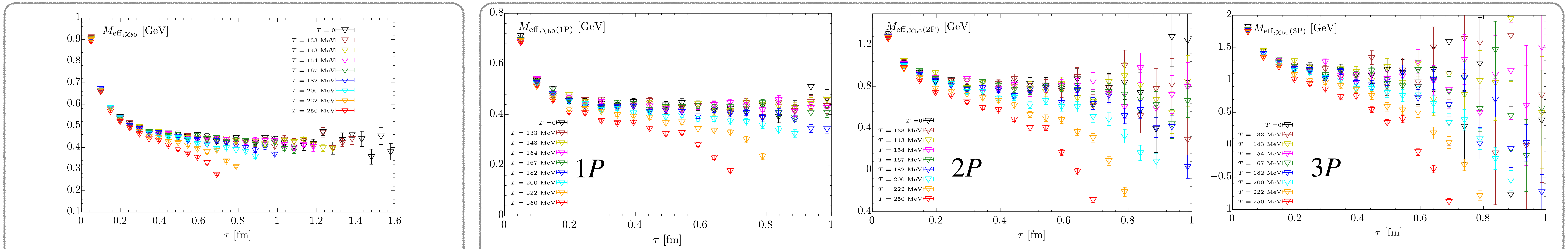

with Gaussian-smeared source

with wave-function optimized source

- No significant changes in in-medium masses
- Sequential thermal broadening

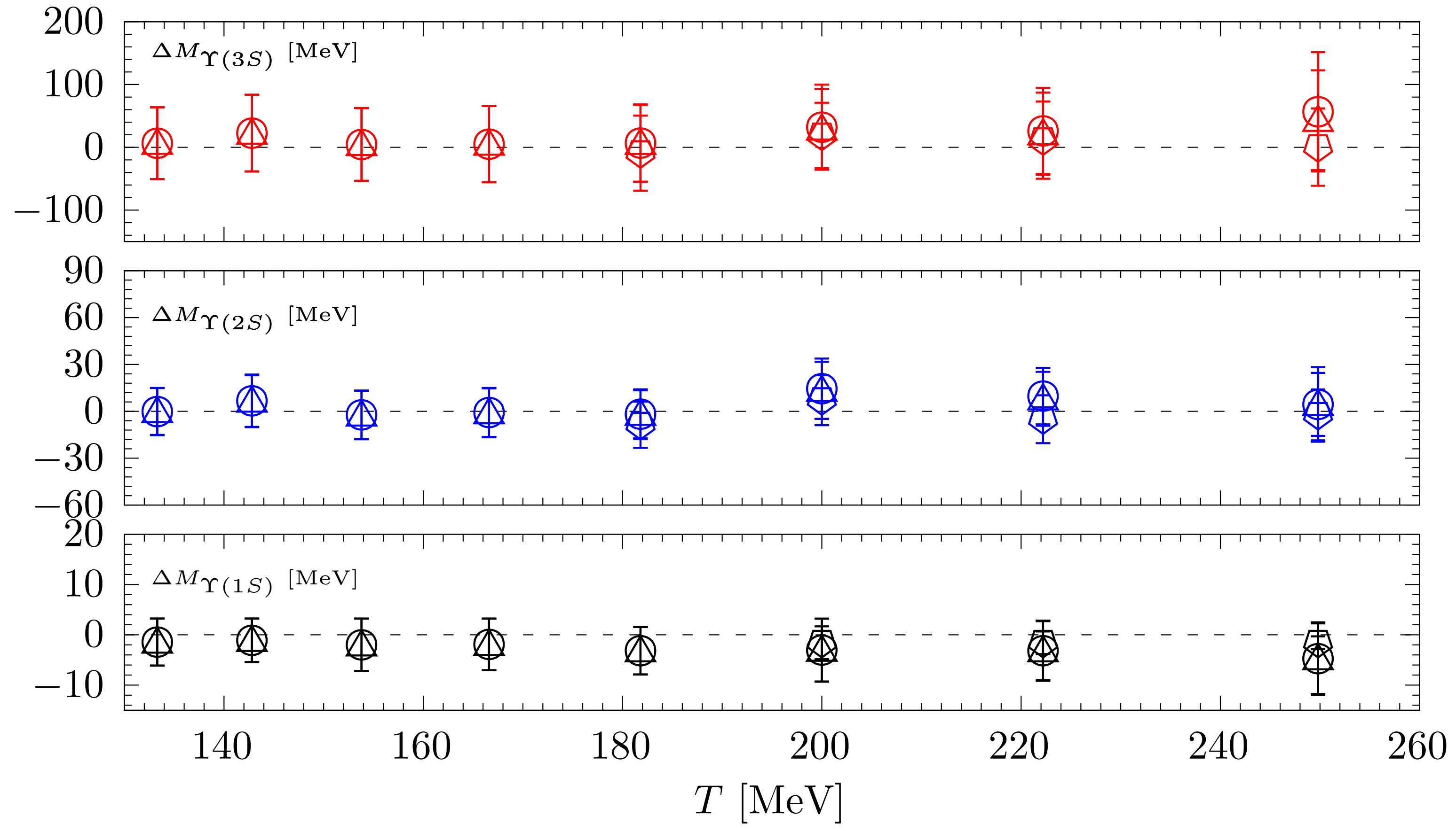

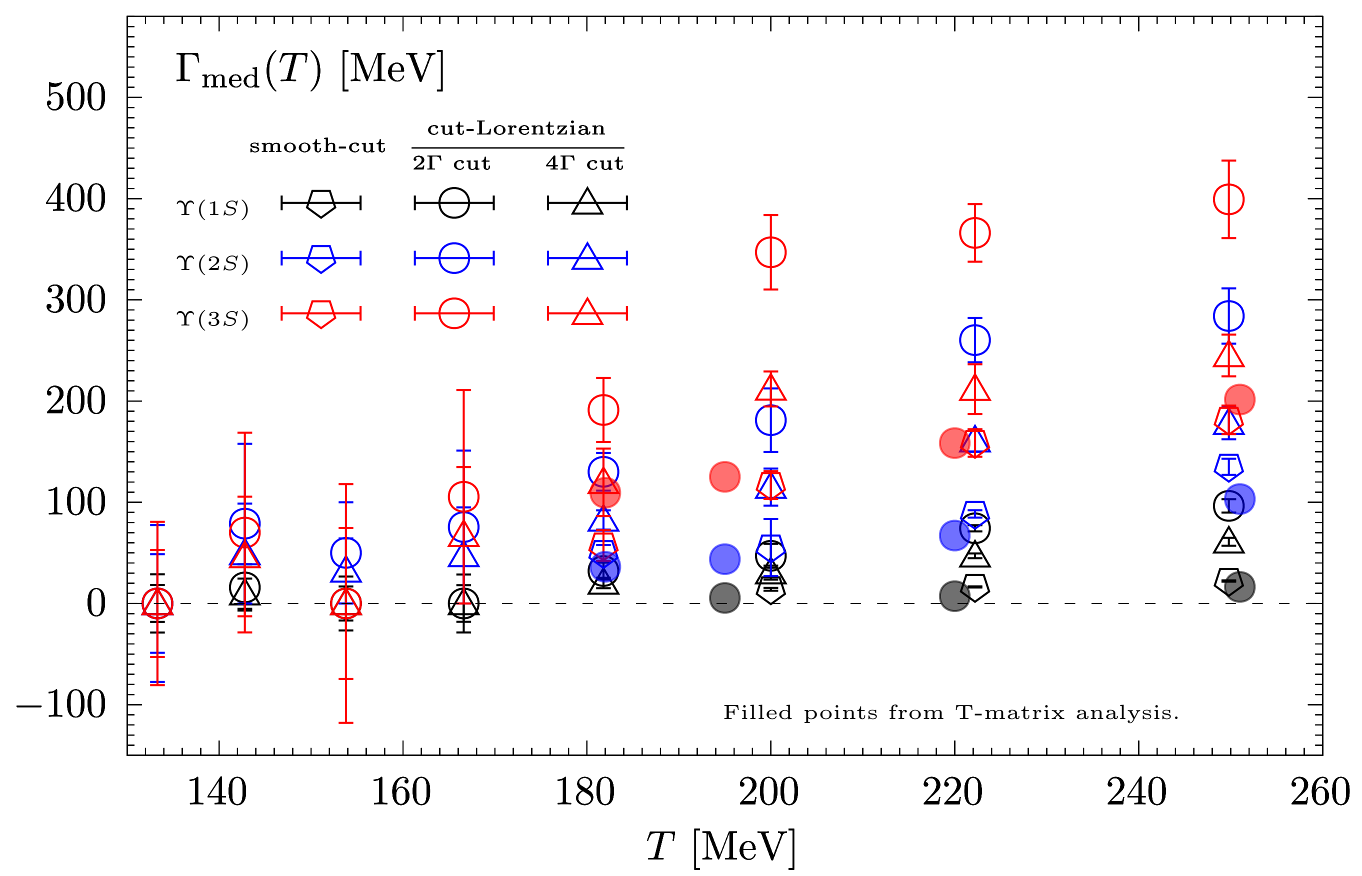

- In-medium modification is not affected by the choices of extended sources

Backup

Ground state extraction

Ground states are extracted by 1-state fits on correlators within $[\tau_{\min},\ \tau_{\max}]$

$\tau_{\max}$: Signal-to-noise ratio reaches to 1% (Gaussian) and 8% (wave-opt.)

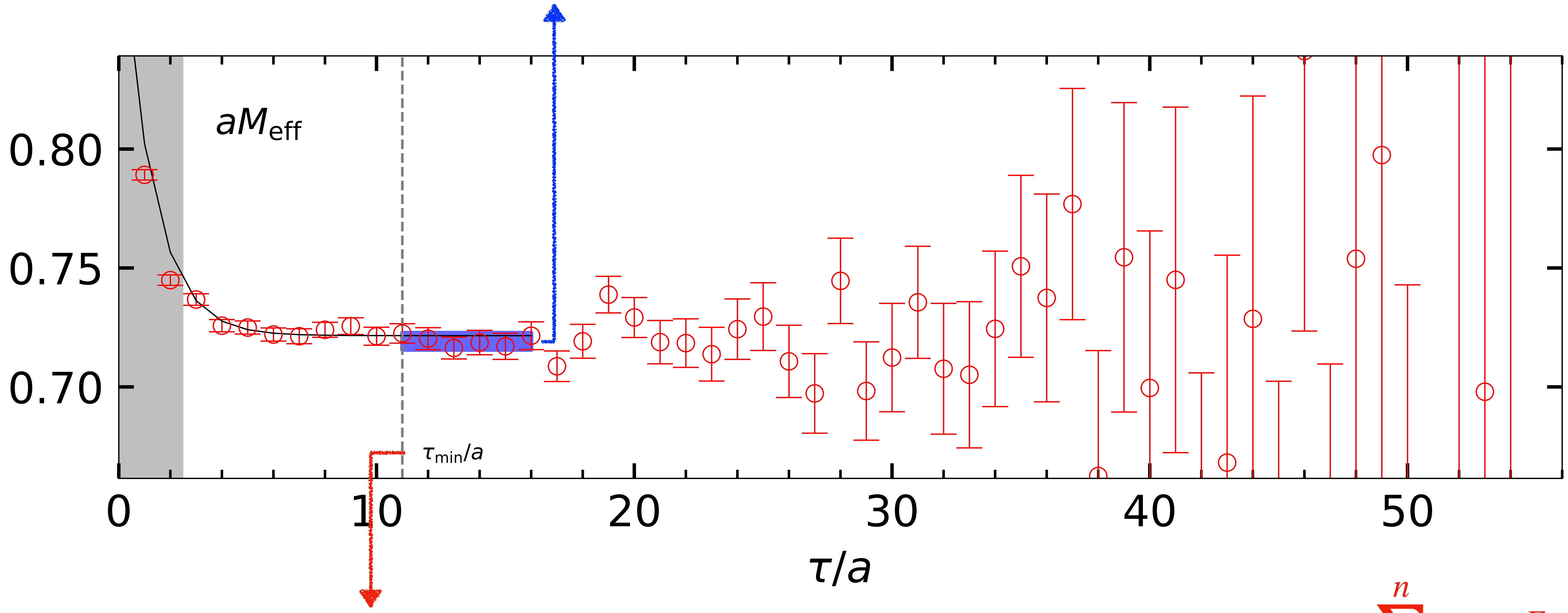

$\tau_{\min}$: 1. Two-state exponential fit to estimate high state contribution via $f_n(\tau) = \sum_{i=0}^{n} A_i e^{-E_i\tau}, n = 1$

2. Excited-state contribution to the effective mass is under statistical uncertainty:

$$\frac{\log[f_1(\tau)/f_1(\tau+a)] - \log[f_0(\tau)/f_0(\tau+a)]}{E_0} < 25\% \times \frac{\delta_{M_{\rm eff}}(\tau)}{M_{\rm eff}(\tau)}$$

P. Fritzsch, et.al., NPB 865, 397(2012)

Bottomonium system from PDG

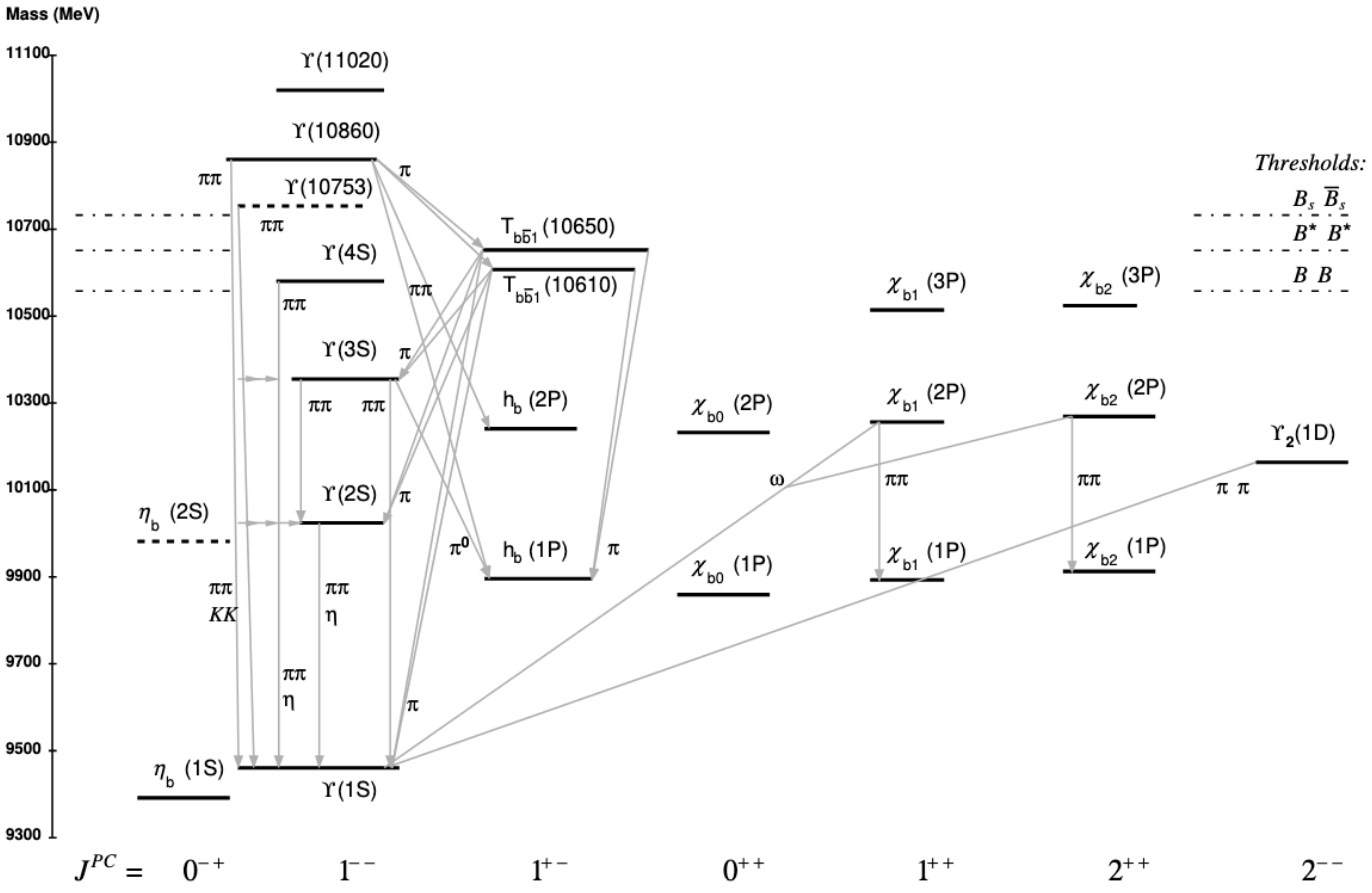

Continuum-subtracted effective mass

Measured with wave-function optimized sources

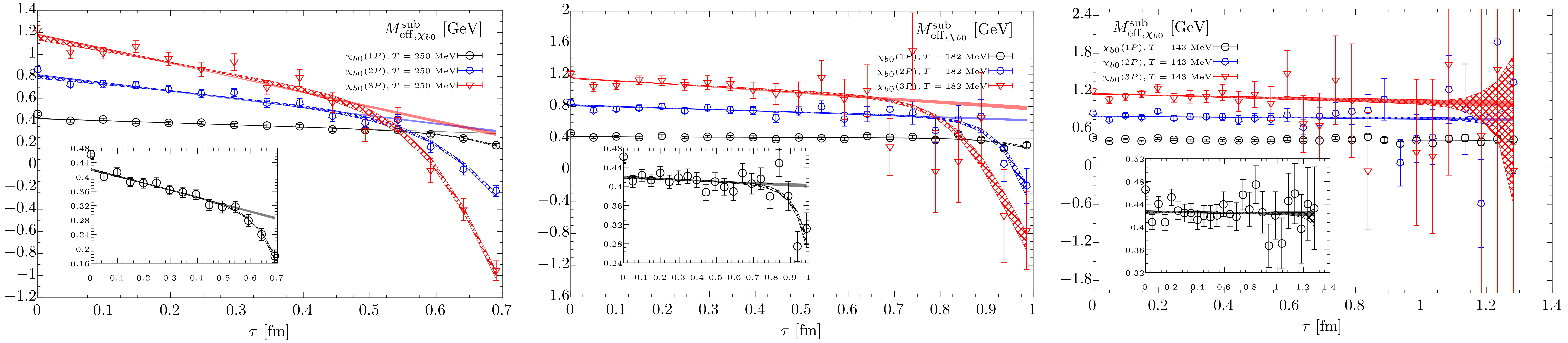

Larger slopes for higher excited states: High excited states are more sensitive to thermal modifications